2nd IBS Conference on Exotic Nuclei, Daejeon, 22-24, July 2026

Universal Width Predictions for Near-Threshold Neutron Resonances

Myungkuk Kim

Center for Exotic Nuclear Studies, IBS

with Y.-H. Song, Y. Kim, H.-W. Hammer, Y. Z. Ma, and D. Lee

Based on arXiv: 2607.14464

Ab Initio Calculations of the Carbon & Oxygen isotopes

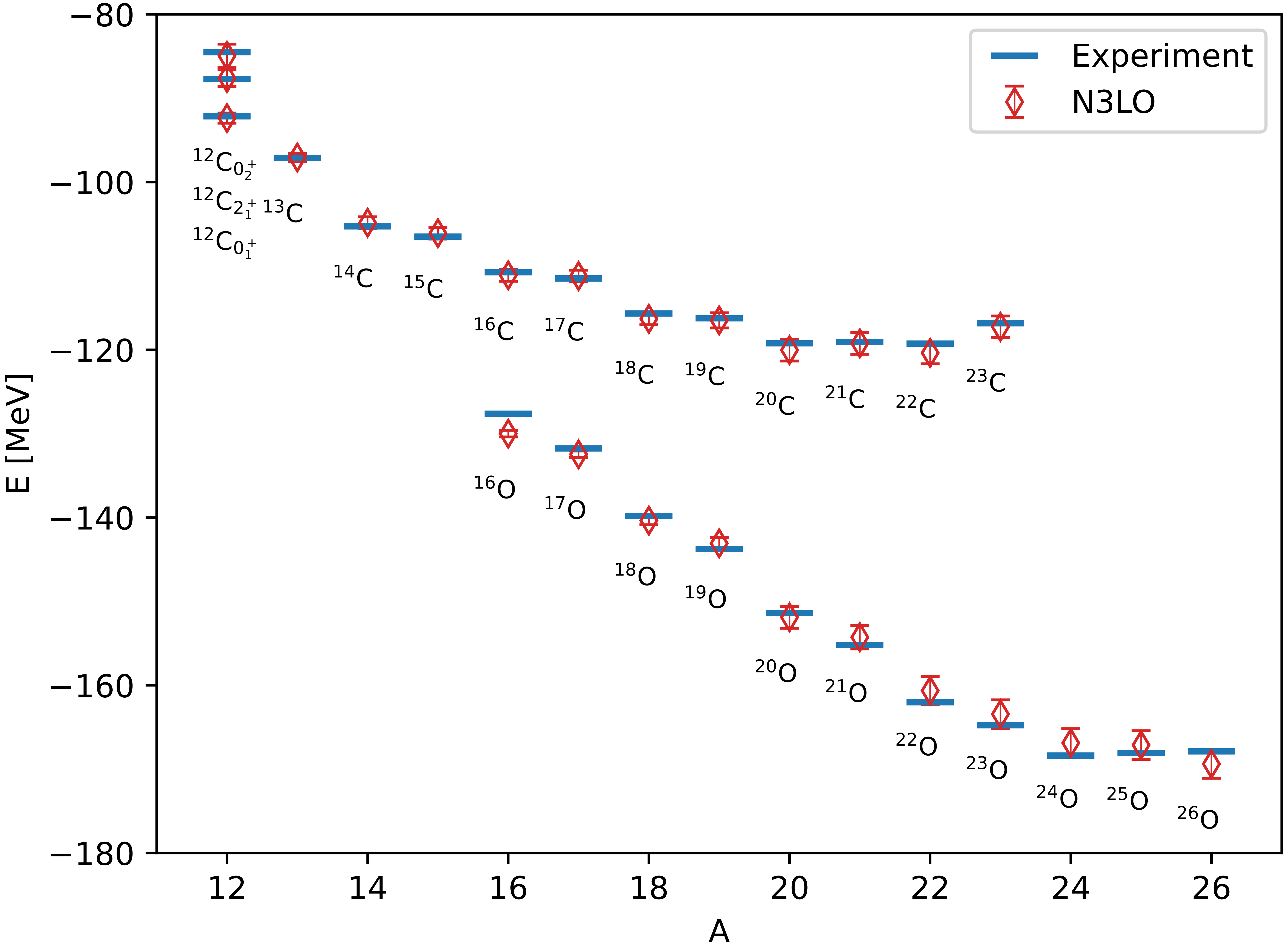

Y.-H Song et al., Phys. Lett. B 872, 140086 (2026)

Neutron dripline & single neutron resonance

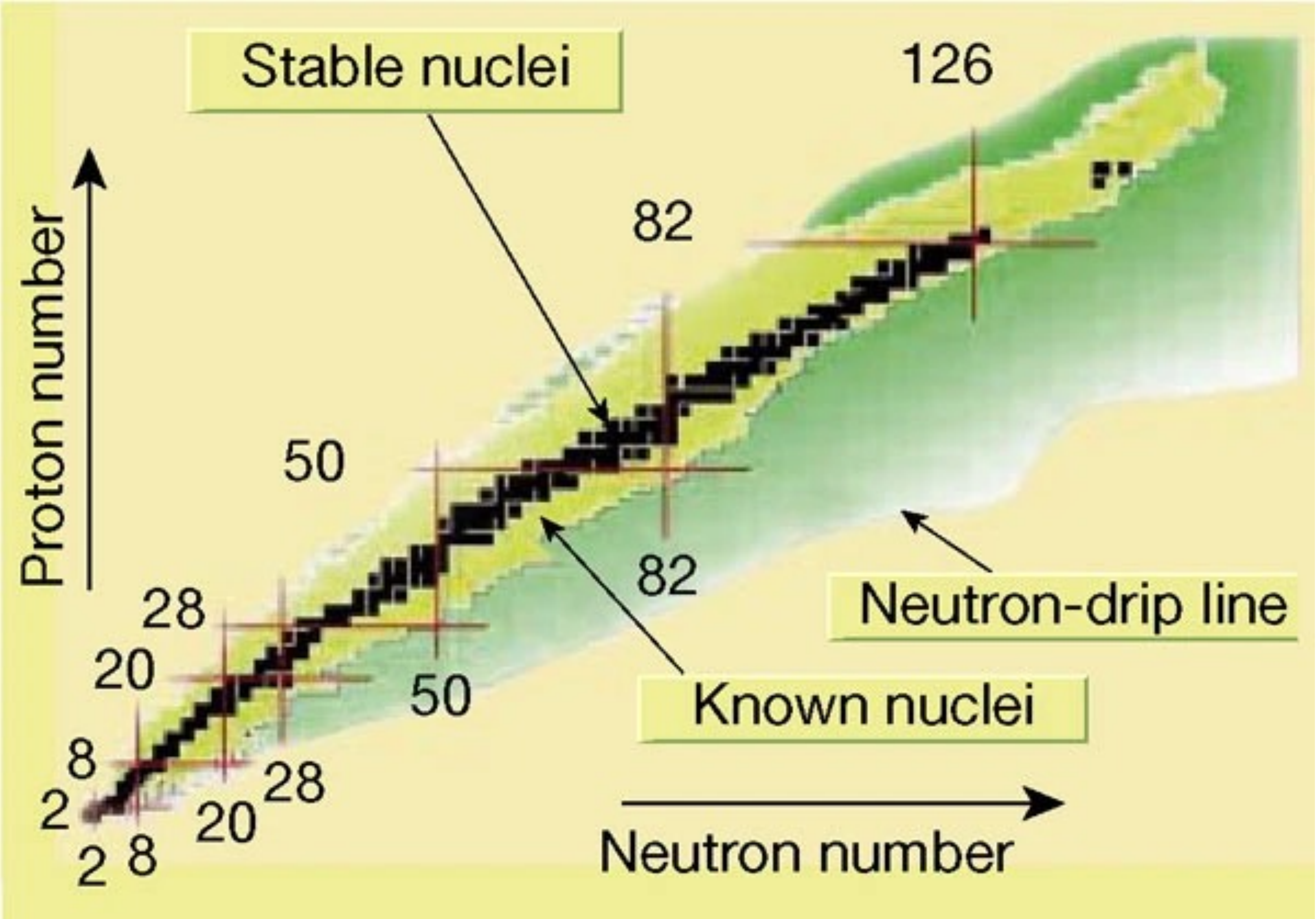

Hellemans, *Nature* **409**, 448–450 (2001)

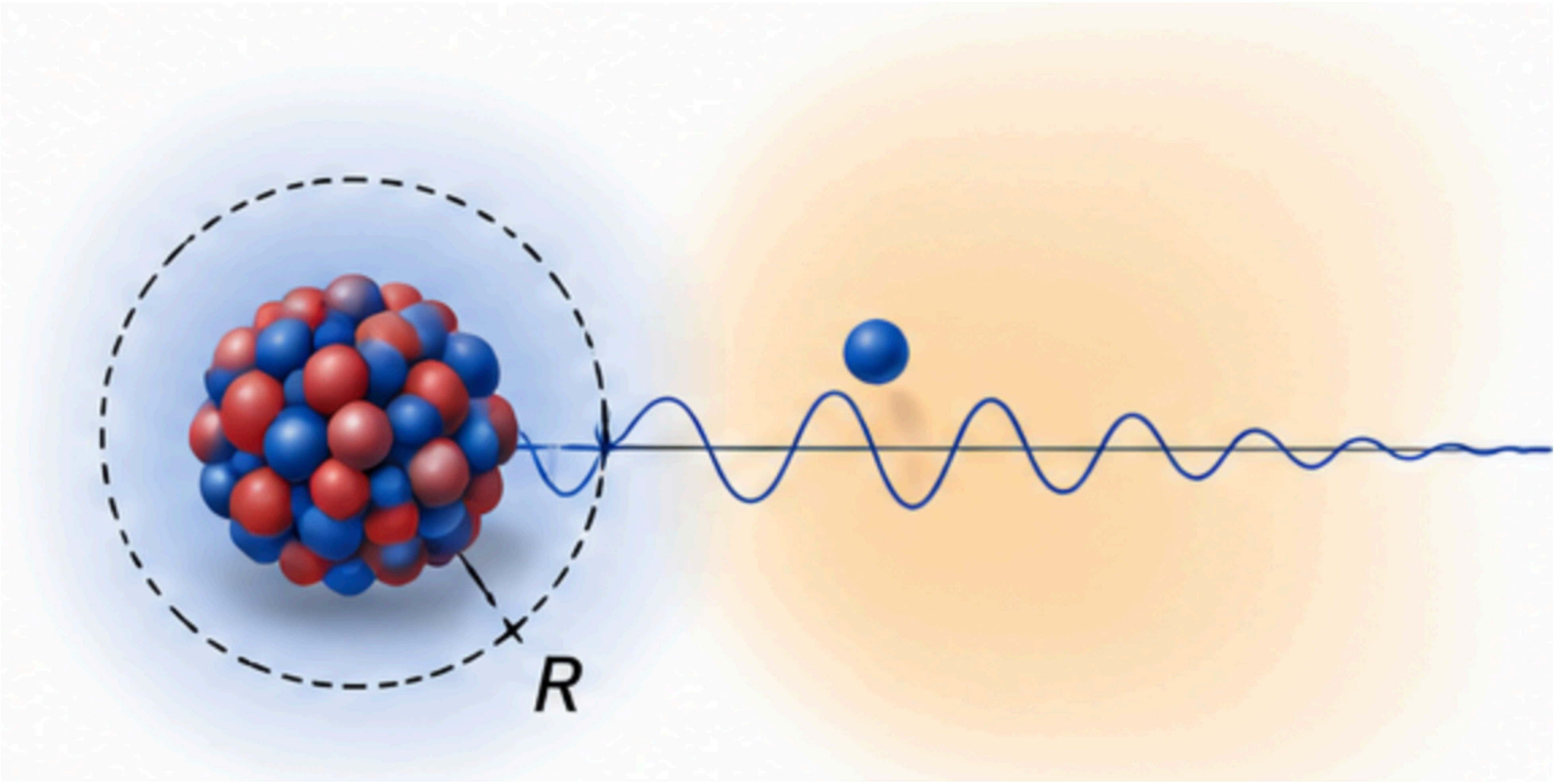

provide a crucial experimental and theoretical window into the extreme realm of the neutron dripline

Universality of single-neutron resonance near-threshold

- Diverging wavelength: As resonance energy approaches zero, the wavelength expands significantly.
- Barrier dominance: Decay dynamics become dictated by the external potential barrier rather than internal structure.
- Interaction decoupling: Short-distance details of strong nuclear interactions decouple from long-range asymptotic behavior.
- Universal constraints: Observables like decay widths are governed by universal geometric constraints than fine details.

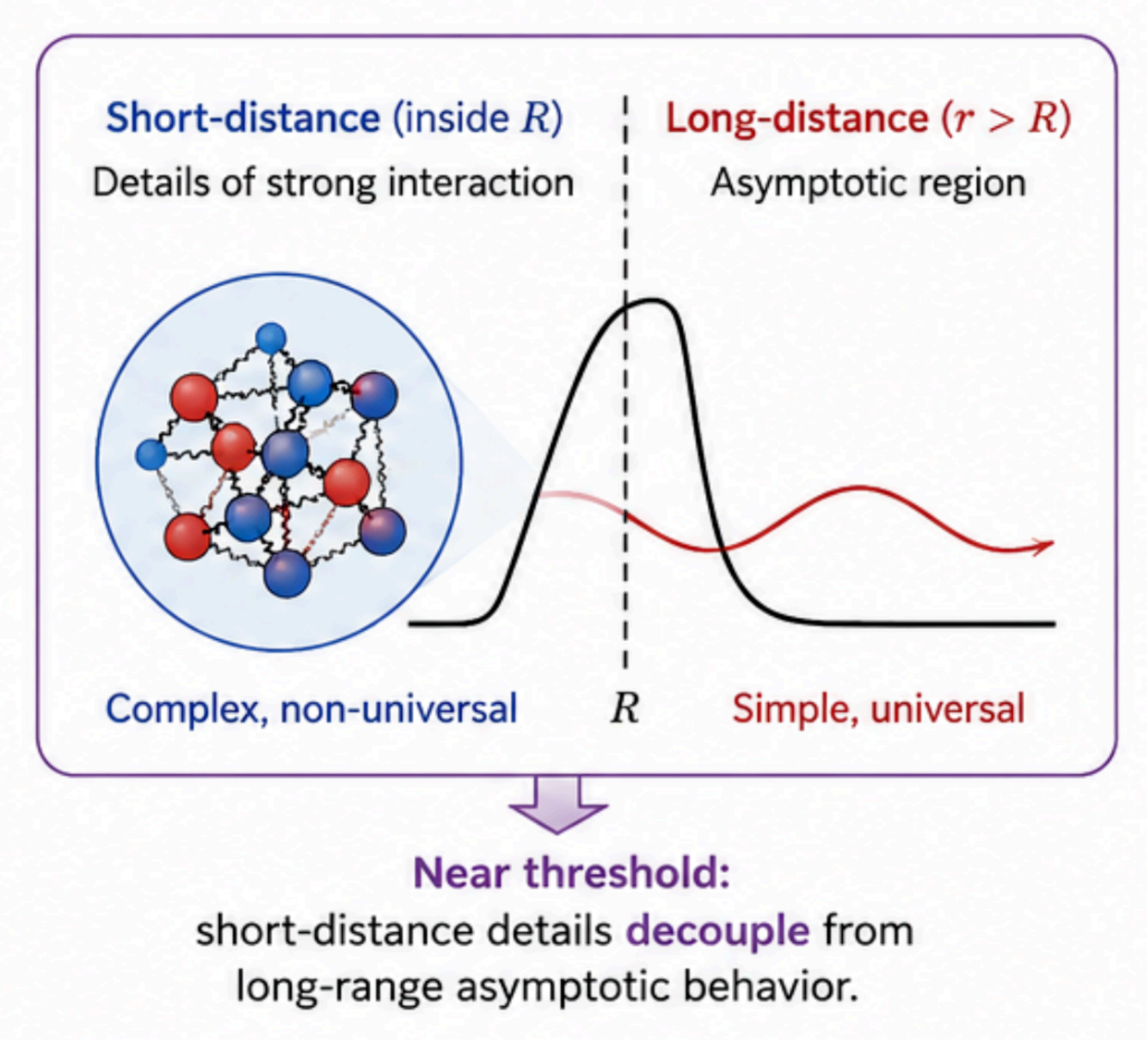

Role of orbital angular momentum (L > 0)

S-wave (L = 0) limits

Neutral s-wave interactions lack a confining barrier, leading near-threshold poles to appear as bound or virtual states rather than shape resonance.

Centrifugal barrier

For L > 0, the centrifugal term provides the vital spatial trapping required to form sharp shape resonances near threshold.

Restricted focus

By restricting studies to systems with at most one charged particle, we isolate universal width scaling for waves with L > 0.

Effective range expansion & Pole relation

- Scattering phase shift for relative momentum is parameterized by the effective range expansion,

$$k^{2L+1}\cot\delta_L(k) = -\frac{1}{a_L} + \frac{1}{2}r_L k^2 + \ldots,$$

- Analytic continuation to the S-matrix pole at $E_{pole} \approx E_r - i\Gamma_L/2$ yields:

$$\Gamma_L \approx 2\frac{k_r^{2L+1}}{\mu|r_L|}$$

Predicting width reduces to determining the effective range

Discrete scale invariance in square wells

- Effective range upper limit: constrained by causality and generalized Wigner bounds, the effective range at zero-energy threshold is bounded by exterior scattering solutions

$$r_L \leq b_L(R) = -\frac{2\Gamma(L-1/2)\Gamma(L+1/2)}{\pi}\left(\frac{R}{2}\right)^{1-2L}$$

H.-W. Hammer and D. Lee, Annals Phys. 325, 2212 (2010)

- Scale-inherent relation: for a square well tuned to threshold, internal wave function normalization links the effective range directly to the exterior geometry:

$$r_L = -\left(L+\frac{1}{2}\right)|b_L(R)|$$

sharpening factor

$$\boxed{\Gamma_L \approx 2\frac{k_r^{2L+1}}{\mu|r_L|} \to \frac{\pi(2\mu E_r)^{L+1/2}\left(\frac{R}{2}\right)^{2L-1}}{\mu(L+1/2)\Gamma(L-1/2)\Gamma(L+1/2)}}$$

Discrete scale invariance & Decoupling of internal dynamics

- Independence from Internal Structure: Discrete symmetry decouples internal radial excitation from external decay dynamics, the potential depth V_0 vanishes from the observable width, making the square-well prediction rely solely on external geometry (independent of *n*).

- Analogy to Quantum Scale Symmetries: The discrete scale invariance of the threshold square-well potential shares similarities with the discrete scale symmetry found in the Efimov effect and relate phenomena.

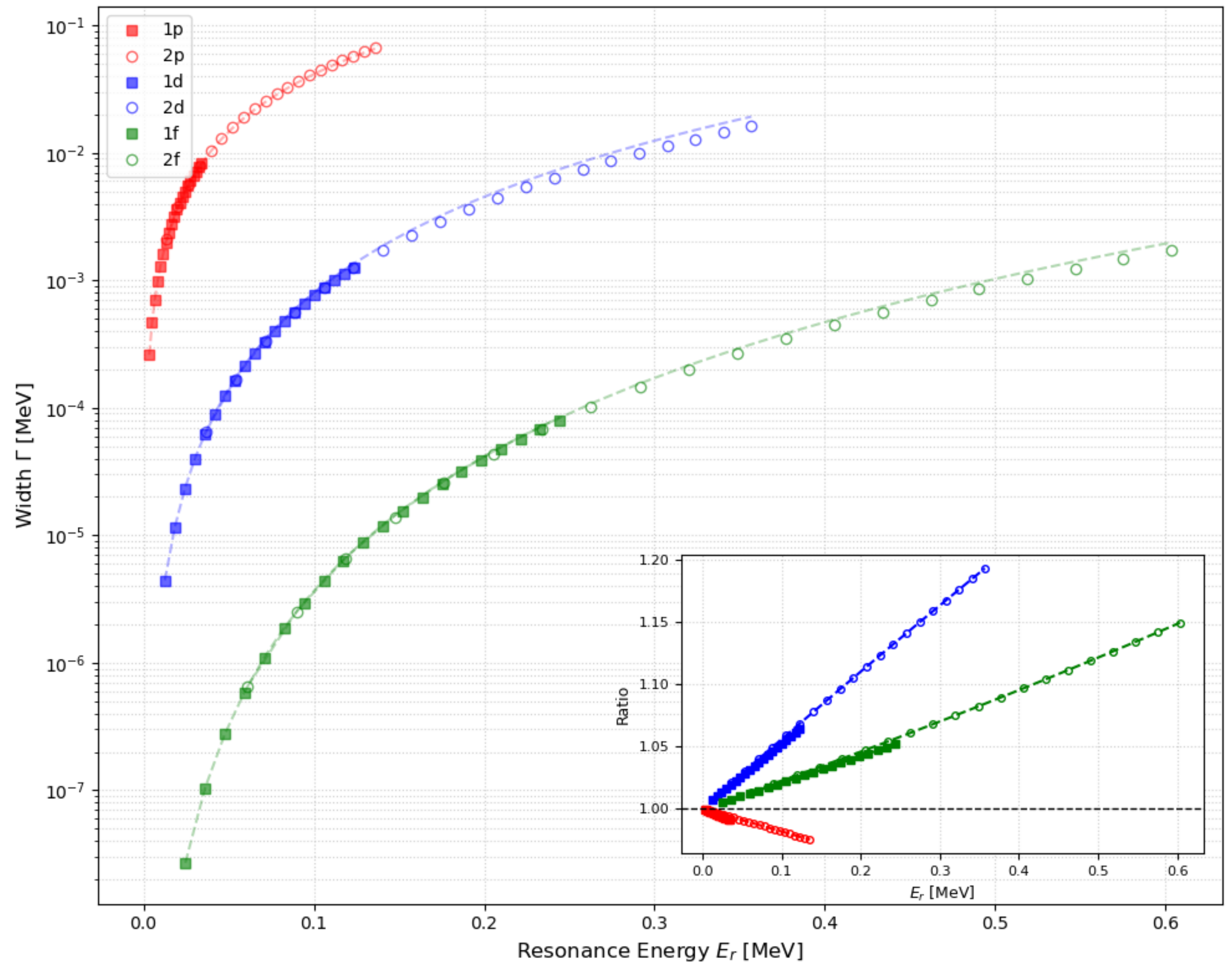

Empirical validation across experimental data

Isotope	J^π	L	A_{core}	R_{eff} (fm)	E_r^{exp} (MeV)	Γ^{exp} (MeV)	Ref.
^{5}He	$3/2^-$	1	4	2.957	0.735(30)	0.719(30)	[27]
^{7}He	$3/2^-$	1	6	3.219	0.430(3)	0.182(5)	[28]
^{9}He	$1/2^-$	1	8	3.428	1.28(1)	0.82(4)	[29]
^{13}Be	$1/2^-$	1	12	3.759	0.51(1)	0.45(3)	[30, 31]
^{28}F	1^-	1	27	4.571	0.199(6)	0.18(4)	[32, 33]
^{11}Be	$5/2^+$	2	10	3.605	1.276(1)	0.10(1)	[34]
^{15}Be	$5/2^+$	2	14	3.897	1.80(10)	0.575(200)	[35]
^{25}O	$3/2^+$	2	24	4.439	0.749(10)	0.088(6)	[36, 37]

$$\Gamma_L = \frac{\pi(2\mu E_r)^{L+1/2}\left(\frac{R}{2}\right)^{2L-1}}{\mu(L+1/2)\Gamma(L-1/2)\Gamma(L+1/2)}$$

$$R_{\text{eff}} = R_0\,(A_{\text{core}}^{1/3}+1) \qquad \frac{4}{3}\pi R_0^3 = \rho_0^{-1}$$

[27] D. R. Tilley, C. M. Cheves, J. L. Godwin, G. M. Hale, H. M. Hayes, J. H. Kelley, C. G. Sheu, and H. R. Weller, Energy levels of light nuclei $A = 5$, 6, 7, Nucl. Phys. A **708**, 3 (2002).

[28] Z. Cao *et al.*, Recoil proton tagged knockout reaction for ^{8}He, Phys. Lett. B **707**, 46 (2012).

[29] Sun, Y. L. and others, Observation of a broad *p*-wave resonant state in ^{9}He, arXiv preprint (2026), arXiv:2602.07810 [nucl-ex].

[30] Y. Kondo *et al.*, Low-lying resonant states in ^{13}Be, Phys. Lett. B **690**, 245 (2010).

[31] A. Corsi *et al.*, Structure of ^{13}Be studied in proton knockout from ^{14}B, Phys. Lett. B **797**, 134843 (2019), arXiv:1908.09459 [nucl-ex].

[32] A. Revel *et al.* (SAMURAI21 collaboration), Extending the southern shore of the island of inversion to ^{28}F, Phys. Rev. Lett. **124**, 152502 (2020).

[33] D. S. Delion and S. Ghinescu, Systematics of neutron emission, J. Phys. G **52**, 055105 (2025), arXiv:2311.08180 [nucl-th].

[34] J. H. Kelley, E. Kwan, J. E. Purcell, C. G. Sheu, and H. R. Weller, Energy levels of light nuclei $A = 11$, Nucl. Phys. A **880**, 88 (2012).

[35] J. Snyder *et al.*, First observation of the unbound nucleus ^{15}Be, Phys. Rev. C **88**, 031303 (2013).

[36] Y. Kondo *et al.*, Nucleus ^{26}O: A Barely Unbound System beyond the Drip Line, Phys. Rev. Lett. **116**, 102503 (2016).

[37] C. R. Hoffman *et al.*, Determination of the $N = 16$ halo shell closure at the oxygen drip line, Phys. Rev. Lett. **100**, 152502 (2008), arXiv:0801.3855 [nucl-ex].

Empirical validation across experimental data

Isotope	J^π	L	$A_{\rm core}$	$R_{\rm eff}$ (fm)	$E_r^{\rm exp}$ (MeV)	$\Gamma^{\rm exp}$ (MeV)	$\Gamma_{\rm SW}^{\rm pred}$ (MeV)	Ref.
^{5}He	$3/2^-$	1	4	2.957	0.735(30)	0.719(30)	0.488(30)	[27]
^{7}He	$3/2^-$	1	6	3.219	0.430(3)	0.182(5)	0.246(03)	[28]
^{9}He	$1/2^-$	1	8	3.428	1.28(1)	0.82(4)	1.371(16)	[29]
^{13}Be	$1/2^-$	1	12	3.759	0.51(1)	0.45(3)	0.385(11)	[30, 31]
^{28}F	1^-	1	27	4.571	0.199(6)	0.18(4)	0.117(05)	[32, 33]
^{11}Be	$5/2^+$	2	10	3.605	1.276(1)	0.10(1)	0.2112(4)	[34]
^{15}Be	$5/2^+$	2	14	3.897	1.80(10)	0.575(200)	0.656(91)	[35]
^{25}O	$3/2^+$	2	24	4.439	0.749(10)	0.088(6)	0.113(04)	[36, 37]

$$\Gamma_L = \frac{\pi(2\mu E_r)^{L+1/2}\left(\frac{R}{2}\right)^{2L-1}}{\mu(L+1/2)\Gamma(L-1/2)\Gamma(L+1/2)}$$

$$R_{\rm eff} = R_0\,(A_{\rm core}^{1/3}+1) \qquad \frac{4}{3}\pi R_0^3 = \rho_0^{-1}$$

[27] D. R. Tilley, C. M. Cheves, J. L. Godwin, G. M. Hale, H. M. Hayes, J. H. Kelley, C. G. Sheu, and H. R. Weller, Energy levels of light nuclei $A = 5, 6, 7$, Nucl. Phys. A **708**, 3 (2002).

[28] Z. Cao *et al.*, Recoil proton tagged knockout reaction for ^{8}He, Phys. Lett. B **707**, 46 (2012).

[29] Sun, Y. L. and others, Observation of a broad *p*-wave resonant state in ^{9}He, arXiv preprint (2026), arXiv:2602.07810 [nucl-ex].

[30] Y. Kondo *et al.*, Low-lying resonant states in ^{13}Be, Phys. Lett. B **690**, 245 (2010).

[31] A. Corsi *et al.*, Structure of ^{13}Be studied in proton knockout from ^{14}B, Phys. Lett. B **797**, 134843 (2019), arXiv:1908.09459 [nucl-ex].

[32] A. Revel *et al.* (SAMURAI21 collaboration), Extending the southern shore of the island of inversion to ^{28}F, Phys. Rev. Lett. **124**, 152502 (2020).

[33] D. S. Delion and S. Ghinescu, Systematics of neutron emission, J. Phys. G **52**, 055105 (2025), arXiv:2311.08180 [nucl-th].

[34] J. H. Kelley, E. Kwan, J. E. Purcell, C. G. Sheu, and H. R. Weller, Energy levels of light nuclei $A = 11$, Nucl. Phys. A **880**, 88 (2012).

[35] J. Snyder *et al.*, First observation of the unbound nucleus ^{15}Be, Phys. Rev. C **88**, 031303 (2013).

[36] Y. Kondo *et al.*, Nucleus ^{26}O: A Barely Unbound System beyond the Drip Line, Phys. Rev. Lett. **116**, 102503 (2016).

[37] C. R. Hoffman *et al.*, Determination of the $N = 16$ halo shell closure at the oxygen drip line, Phys. Rev. Lett. **100**, 152502 (2008), arXiv:0801.3855 [nucl-ex].

Resonance decay width scaling

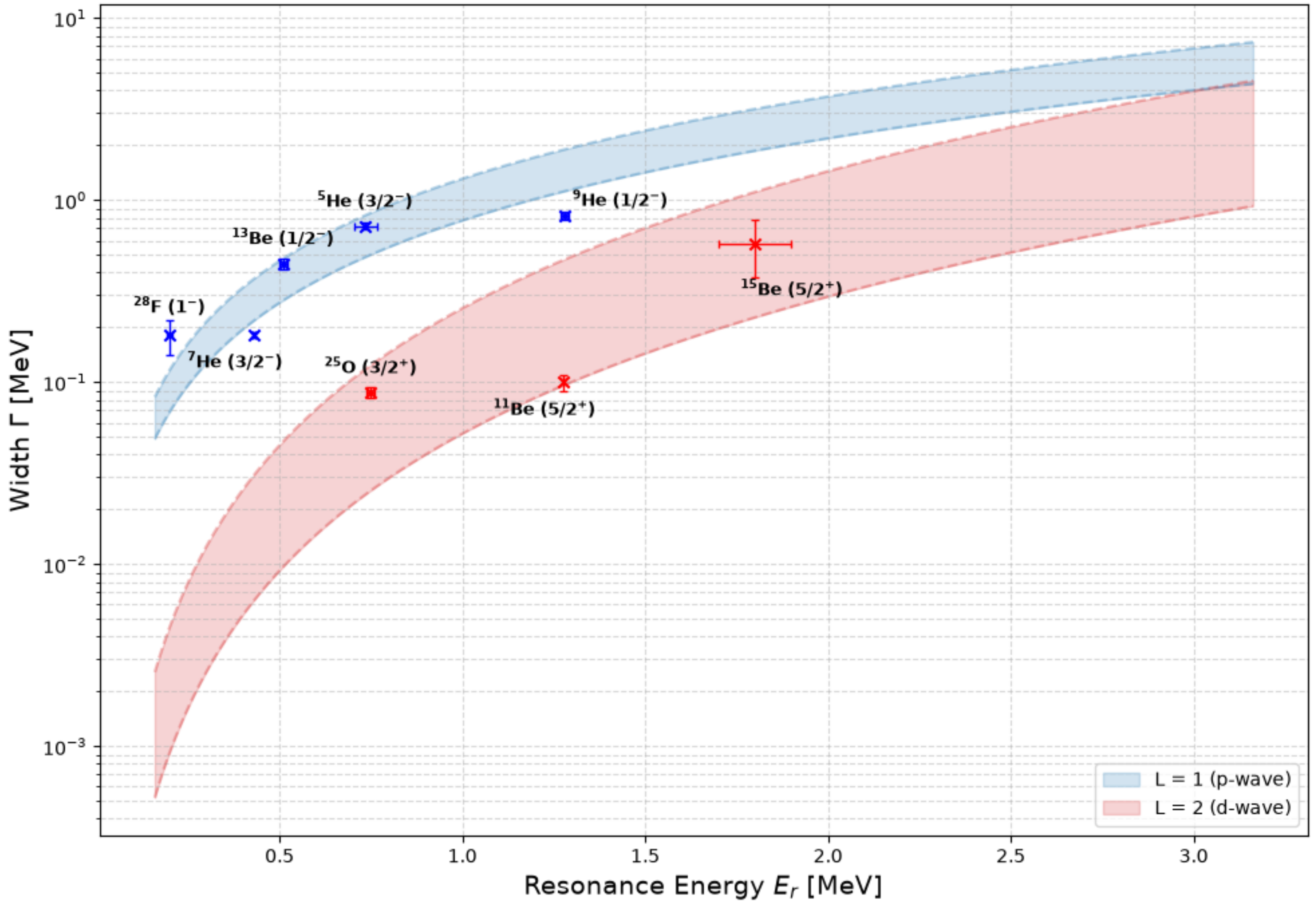

- Experimental data within the band is considered consistent with single-particle behavior.
- Serve as diagnostic tool for identifying collective or non-single-particle nuclear structure effects.
- Within bands, Γ primarily determined by the centrifugal barrier penetration (valence nucleon orbiting a core).
- Evidence for physics beyond the single-particle approximation.

Predictions of resonance decay widths

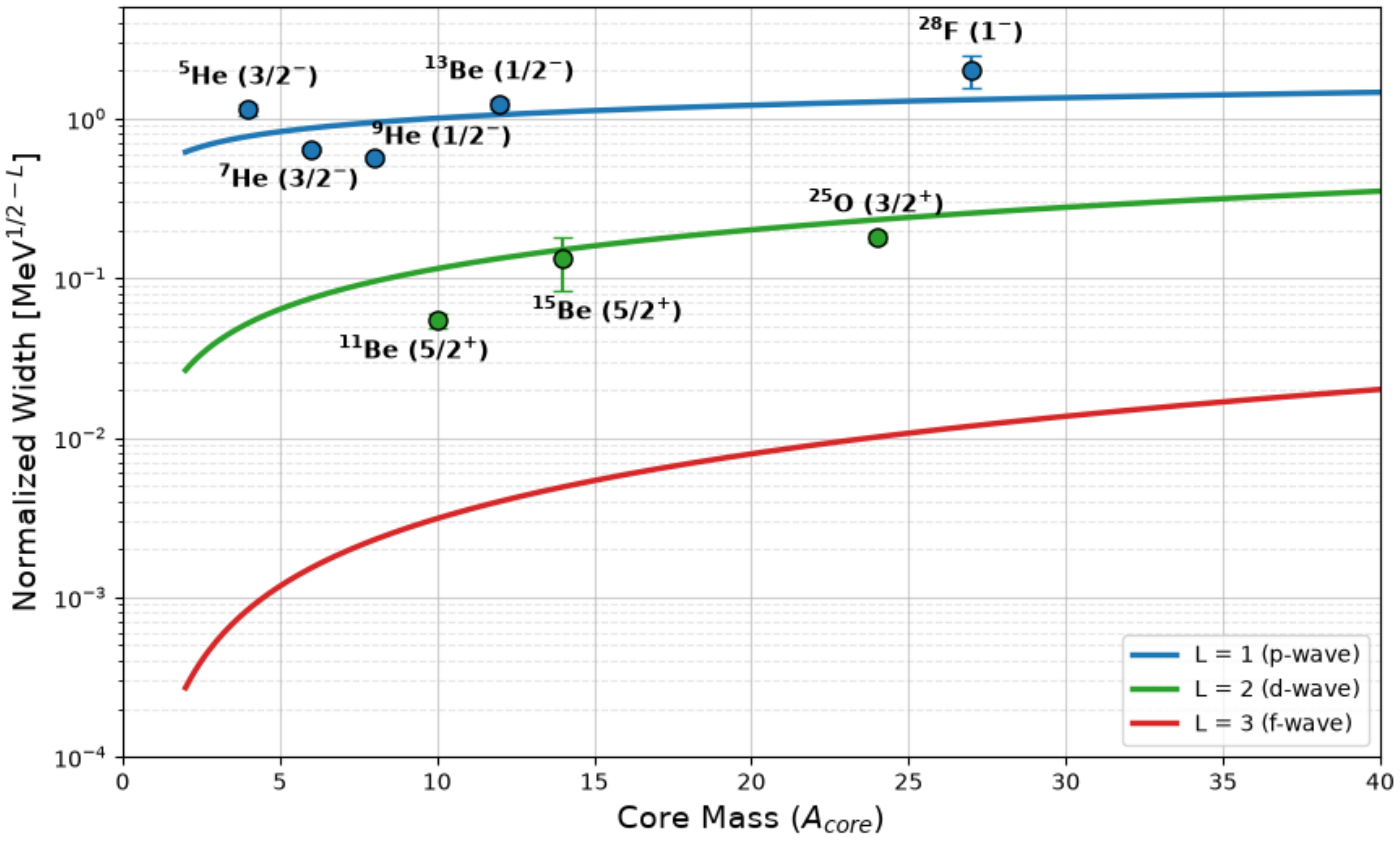

- Robust phenomenological baseline which is governed entirely by the geometric bounds and reduced mass of the system.
- Consistent with Wigner's prediction of the cross section behavior near threshold.
- Threshold decay behavior of a single-neutron state is bounded by the universal properties of the potential.

Conclusions & Summary

- **Universal Geometric Baseline**: Established a scale-invariant square-well baseline for $L > 0$ near-threshold resonances, yielding a closed-form decay width formula dependent solely on geometry, orbital angular momentum, and resonance energy.

- **Discrete Scale Invariance**: Proved that finite square-well potentials exhibit zero-energy discrete scale invariance, which completely eliminates internal radial node sensitivity and potential depth dependencies in the sharp-boundary limit.

- **Diagnostic Utility**: Demonstrated that the framework successfully captures the physical scale of experimental widths within a factor of two, offering a parameter-free spectroscopic benchmark to separate universal threshold continuum physics from complex many-body effects near the neutron dripline.